ELSEVIER

Polymer 43 (2002) 5187–5195

polymer

www.elsevier.com/locate/polymer

Microdomain structure and chain orientation in polypropylene/polyethylene blends investigated by micro-Raman confocal imaging spectroscopy

S. López Quintana[a], P. Schmidt[b,*], J. Dybal[b], J. Kratochvíl[b], J.M. Pastor[c], J.C. Merino[a,c]

[a]*Automotive Research and Development Centre CIDAUT, 47151 Boecillo, Valladolid, Spain*
[b]*Institute of Macromolecular Chemistry, Academy of Sciences of the Czech Republic, Heyrovský Sq. 2, 162 06 Prague, Czech Republic*
[c]*Department of Physics of Condensed Matter, University of Valladolid, 47011 Valladolid, Spain*

Received 5 February 2002; received in revised form 11 June 2002; accepted 12 June 2002

Abstract

Compositional domain structure of blends of isotactic polypropylene with linear polyethylene and chain orientation of neat polymers and of the blends were assessed by micro-Raman confocal imaging spectroscopy and FT Raman spectroscopy. The results were correlated with polarised photoacoustic FTIR and with DSC. The surface and inner parts of compression-moulded, injection-moulded and drawn specimens were compared. Polymer domains in the blends and domains of different orientation were identified. The larger size of the polymer domains and lower chain orientation in the core of the specimens prepared by injection-moulding were explained by different cooling conditions of the melt. Possibilities and limitations of the micro-Raman confocal spectroscopy method were discussed.

Keywords: Micro-Raman confocal spectroscopy; Polypropylene/polyethylene blends; Morphology

1. Introduction

The importance of the domain size and of the chain orientation in polyolefins for their mechanical behaviour is generally well known and the understanding of their morphology on the microscopic scale is very desirable. Optical microscopy cannot discern between polypropylene (PP) and polyethylene (PE) in blends, whereas staining of the blend must be used for such discrimination by electron microscopy.

The potentials of micro-Raman confocal spectroscopy for elucidation of the structure of polymers have been already shown [1–4]. It allows to discern between the polymer domains in the bulk material of the blends on microscopic level down to the spatial resolution of ~2 μm. In addition to the size and shape of domains of the blend components, the orientation of polymer chains in different microregions can also be investigated by the method [5]. As a proper model for such an investigation, we used a 50/50 blend of PP/PE, prepared in the form of compression-moulded, injection-moulded, and injection-moulded subsequently drawn test-pieces.

2. Experimental

2.1. Materials and specimens

Isotactic polypropylene (PP) was Mosten 58412, high-density polyethylene (PE) was Liten MB 62 (both Chemopetrol, Czech Republic). The experimental model blend was prepared by mixing PP and PE pellets (mass ratio 50/50) in a Banbury mixer and then in a double-screw extruder. The standard dumbbell specimens were prepared by injection-moulding. Processing conditions for specimen preparation were described elsewhere [6]. The gauge length, width and thickness of the injection-moulded dumbbell specimens were 90, 10, and 4 mm, respectively. Such specimens were then drawn at 23 °C at a test speed of 20 mm min^{-1} using an Instron 6025. The drawing was heterogeneous, i.e. concentrated in a sharp neck shoulder. The obtained draw ratio reached the value of 5.1. For comparison, macroscopically non-oriented specimens were

* Corresponding author. Tel.: +420-2-20403381; fax: +420-2-35357981.
E-mail address: schmidt@imc.cas.cz (P. Schmidt).

0032-3861/01/$ - see front matter
PII: S0032-3861(02)00384-1

prepared by compression-moulding at a temperature of 220 °C.

2.2. Measurements

Micro-Raman confocal Labram device from Dilor S.A. (Lille, France) was used for Raman confocal measurements. This device uses a He–Ne laser beam operating at 632 nm which delivers ca. 16 mW at the sample surface. The scattered light was detected with a CCD camera. Pinhole apertures (100 μm) and 1800 grooves mm^{-1} grating were used. The spectral resolution was 4 cm^{-1}.

The skin of the material was measured on the surface of the narrower parts of the specimens. For characterisation of inner parts of the material (core), small pyramid-like pieces were cut from the middle of the specimens, with the bases perpendicular to the main plane of the dumbbell. To minimise the damage due to the cutting technique, cut surfaces prepared with an ultramicrotome (Ultrotome III, LKB) were used. The ultrathin sectioning was performed under cryogenic conditions, which is a usual technique in electron microscopy (TEM). The size of the upper plane of the pyramid used for the micro-Raman measurement was ~200 μm × 200 μm.

Point-by-point mapping was carried out using a motorised scanning stage controlled by computer software Labspec (Dilor S.A.). For the formation of polymer domain images, areas 15 μm × 15 μm with the point distance of 0.5 μm were measured with the 100 × magnifying objective. Chain orientation was estimated by mapping the samples in two mutually perpendicular positions so that the direction of injection-moulding and drawing of the specimens were parallel (0°) or perpendicular (90°) to the polarisation of the laser beam. Neither a half-wave plate nor an analyser was used. The data were sampled with the objective magnifying 50 × from the 100 μm × 100 μm squares in steps of 10 or 20 μm. In such a relatively large area, it was necessary to adjust the focus manually.

Polarised FT Raman spectra were measured on a Bruker FT spectrometer IFS 55 equipped with a Raman module FRA 106 at 4 cm^{-1} resolution. The spectra were obtained using a 1064 nm diode-pumped Nd^{+}/YAG laser radiating a horizontally polarised beam of 500 mW. All specimens were positioned with their largest planes perpendicular to the laser beam direction; the lengths of dumbbells (i.e. the direction of injection-moulding and drawing) were oriented vertically. The spectra were obtained from the centre of a dumbbell specimen in the back-scattered regime, in pairs of parallel or perpendicular positions of the half-wave plate with respect to injection-moulding and drawing. An analyser was not used. The positions of samples and the laser intensity were sufficiently stable, so that absolute intensities of two consecutive measurements could be compared.

DSC measurements were carried out on a Perkin Elmer Pyric 1 DSC apparatus. A value of 206 J g^{-1} was used as heat of fusion of 100% crystalline PP [7].

3. Results and discussion

3.1. Polymer domain structure of PP/PE blends

3.1.1. FT Raman spectroscopy

After blending and extrusion, isotactic polypropylene (PP) and linear polyethylene (PE) form immiscible blends, both the components of which show characteristic Raman spectra. As the Nd^{+}/YAG laser beam of the normal FT Raman instrument incident on the polymer has a diameter of ~200 μm and penetrates deep into the material, an information is taken from the optical volume which is much larger than the mean volume of the PP and PE domains present in the blend. As a result, the obtained spectra of the blend are averaged both along the direction and across the thickness of the laser beam.

From Fig. 1 and in accordance with Ref. [8] it follows

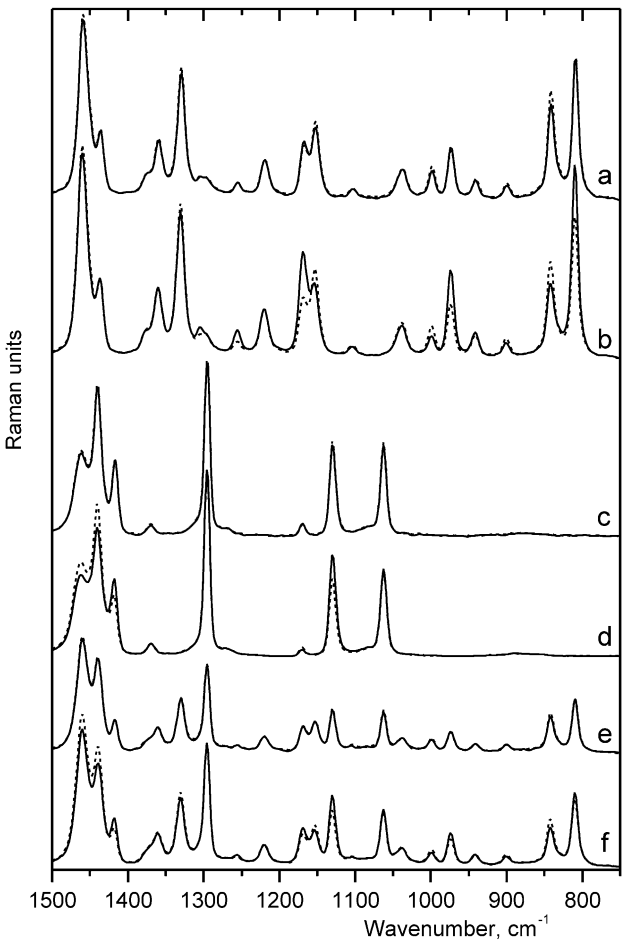

Fig. 1. FT Raman spectra of (a) injection-moulded PP, (b) drawn PP, (c) injection-moulded PE, (d) drawn PE, (e) injection-moulded PP/PE 50/50 blend, (f) drawn PP/PE 50/50 blend. Direction of laser polarisation (—) parallel, (- - -) perpendicular to injection-moulding and drawing direction.

that the bands at 809, 842, and 1330 cm^{-1} characteristic of PP are almost not influenced by the spectrum of PE and, vice versa, the bands 1062, 1130, and 1295 cm^{-1} characteristic of PE are only slightly affected by the PP spectrum [9]. Therefore, the bands at 1330 and 1295 cm^{-1} were chosen for characterisation of domains of PP and PE, respectively, by micro-Raman confocal spectroscopy.

3.1.2. Micro-Raman confocal spectroscopy in the skin and in the core

The point-by-point mapping of the material was made both for the skin and, after removing the skin, for the core. In the micro-Raman confocal mapping, the overall intensity of the Raman signal strongly depends on focusation of the microscope and it cannot be maintained stable for measurements at different points. Consequently, only the ratios of intensities of the Raman bands measured at particular points of the material can be estimated.

Contrary to the normal FT Raman, the micro-Raman confocal measurements yield information from a limited optical volume. With an objective magnifying 100 ×, it has the dimensions of ~2 μm in diameter and of ~2 μm in depth, so that thin layers can be investigated—either directly on the surface or, after cutting the surface off, in the inner part of the material. We have used those measurements for investigating the domain structure of compression-moulded, injection-moulded, and the injection-moulded and subsequently drawn specimens of the PP/PE blend.

In a preliminary micro-Raman confocal examination of differently prepared specimens of the PP/PE 50/50 blend, the PP or PE domains 2–5 μm in size were found. Therefore, the material was characterised by mapping the squares 15 μm × 15 μm, in the steps of 0.5 μ. As isotactic PP and high-density PE are immiscible, only domains of virtually neat PP and PE can exist in the blend. However, due to the final spatial resolution of the instrument (here with the limit of ~2 μm × 2 μm × 2 μm), the boundaries between the PP and PE domains are not sharp in the measured image. With the laser beam focused on the centre of a sufficiently large domain, the spectrometer should record the presence of an individual polymer only. The smaller the polymer domains are, the stronger Raman intensity from the other polymer reaches the detector and the lower are the composition differences between the spectra taken at different points of the material. PP or PE domains smaller than 1 μm cannot be discerned by the micro-Raman confocal method at all.

The results are documented in Fig. 2 consisting of six spectral images of 15 μm × 15 μm squares. The images are presented in the three-dimensional recalculated form. The integral intensity ratio of 1330 and 1295 cm^{-1} bands obtained from the mean spectrum of the measured square was used for recalculation, so that the vertical axes of the images correspond to the average fraction of PP detected in a particular position. In addition, two extreme Raman spectra were extracted for each image, corresponding to the 'PP-rich' and 'PP-poor' locations.

In Fig. 2, some differences between the size of the PP and PE domains in different specimens can be seen. The largest domains (~10 μm) are located inside the compression-moulded samples (a) and slightly smaller domains are on their surfaces (b). Then, the inner part of the injection-moulded sample follows, with the medium domain size (c). The domains of the core are slightly more ordered in the direction of subsequent specimen drawing (e). The differences between the PP-rich and PP-poor spectra extracted from these images are substantial.

The polymer domain structure of the surfaces (skins) of the samples prepared by injection-moulding is comparatively fine. On the surfaces of the injection-moulded as well as of injection-moulded and subsequently drawn samples the PP and PE microdomains are smaller than 2 μm, which is the spatial resolution of micro-Raman confocal spectroscopy (see Fig. 2(d) and (f)). This causes at the same time lower differences in the intensity shown in the vertical axis of the image—the domains are almost indiscernible. The spectra extracted from the slightly 'PP richer' and 'PP poorer' locations of the skin are almost identical.

We tried to obtain some information about the thickness of the skin layers of injection-moulded dumbbell specimens by focusing the laser deeper into the material. The spectra with a reasonable *S/N* ratio could be obtained up to the depths of ~25 μm. The obtained images showed that the skin of the specimens with fine domain structure is thicker than that value.

The existence of a specific skin structure on the surfaces of injection-moulded specimens is caused by a rather rapid cooling of the material on the surfaces of injection-moulded dumbbells, so that the material retained its fine structure obtained after mixing the melt. On the other hand, the material inside the injection-moulded dumbbells and in the compression-moulded plates remained for a longer time in the molten state and a separate coalescence of PP and PE drops could proceed.

3.2. Chain orientation structure

3.2.1. FT Raman spectroscopy

A comparison of intensities of oppositely polarised PP bands at 842 and 809 cm^{-1} suggests the possibility of estimating roughly the orientation of PP chains. In the back-scattered Raman experiment, the intensity ratio I_{842}/I_{809} is minimal if the chains are parallel to the laser polarisation and reaches a maximum value if the chains are perpendicular to the polarisation [8]. As could be expected, with the compression-moulded specimens, no preferred average chain orientation was found. Fig. 1 shows that the spectra of the injection-moulded PP, both neat and blended, show also no or only very small differences between the intensity ratios of 842 and 809 cm^{-1} bands at opposite orientation of the laser polarisation with respect to the injection direction.

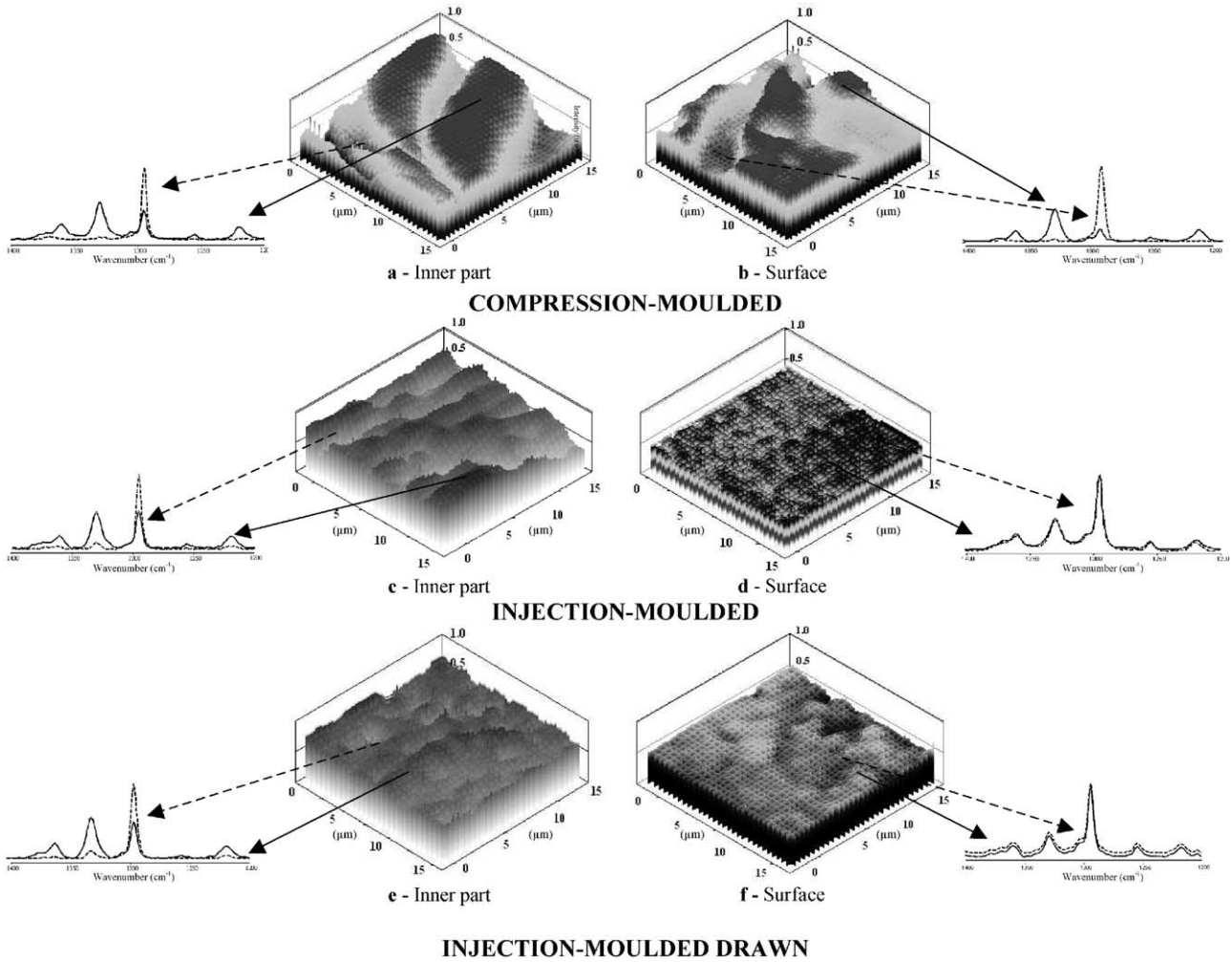

Fig. 2. Micro-Raman images of the PP/PE 50/50 blends. Squares 15 μm × 15 μm, objective magnifying 100 × . (a) Inner part of compression-moulded, (b) surface of compression-moulded, (c) inner part of injection-moulded, (d) surface of injection-moulded, (e) inner part of injection-moulded and drawn, (f) surface of injection-moulded and drawn specimen. Micro-Raman spectra of PP-rich sites (—) extracted from the top and of PP-poor sites (- - -) extracted from the depression of the images.

Only after drawing, the usual Raman spectra manifest a uniaxial orientation of PP chains. Similarly, the formation of an optical anisotropy can be seen for the Raman bands of neat PE and PE in the blend only after plastic drawing. Nevertheless, in all the mentioned cases, the influence of depolarisation of the bands by scrambling of the laser beam and of the Raman radiation on the optical inhomogeneities of the material must be taken into account even for a rough estimation of orientation [8]. The measured optical anisotropy of the material can strongly decrease as a consequence of such a scrambling, which could fully distort the conclusions about the chain orientation of the material.

3.2.2. Micro-Raman confocal spectroscopy

3.2.2.1. Separate estimation of average orientation in the skin and in the core. Contrary to the usual FT Raman spectroscopy, in the micro-Raman confocal measurements the penetration depth of the laser beam has fixed limits providing information on a limited optical volume. As a result, the chain orientation in the skin and in the core of the material can be estimated separately.

As mentioned above, the absolute intensities of the signal of the micro-Raman confocal spectra depends strongly on the focusation of the beam. Because of this, the absolute intensities of the bands measured in different points of the sample cannot be compared and the chain orientation of the material in different positions and/or at different sample orientation can be characterised only by the intensity ratios of the oppositely polarised Raman bands.

For the characterisation of the orientation of PP chains at individual sites, the intensity ratio of the oppositely polarised PP Raman bands at 809 and 842 cm^{-1} was used. In our preliminary micro-Raman confocal mapping of polyolefin materials, the existence of domains of the size 15–50 μm showing different directions of chain orientation was found. Hence, the mean orientation in the skin and in the core of the materials was characterised comparing the

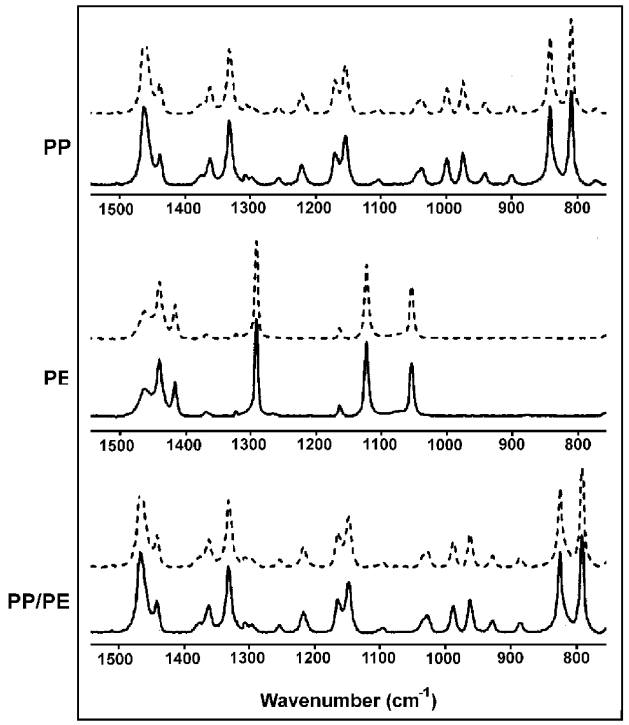

Fig. 3. Micro-Raman confocal mean spectra of compression-moulded neat PP, neat PE and PP/PE 50/50 blend measured at two opposite directions in a $100 \times 100\ \mu m^2$ square, objective magnifying $50\times$. Direction of laser polarisation (—) parallel, (- - -) perpendicular to the assumed flow of material during compression moulding.

intensities of the oppositely polarised 809 and 842 cm^{-1} bands of the mean spectra, obtained by averaging the measurements of the squares $100 \times 100\ \mu m^2$ mapped point-by-point with a $50\times$ magnifying objective in steps of 10 or 20 μm. In such a way, the micro-Raman confocal mean spectra of neat PP, neat PE and of PP/PE blend of pressed specimens and of the core and skin of injection-moulded and drawn specimens were measured.

Figs. 3–5 show 15 pairs of the mean spectra, each pair measured in two opposite directions—parallel and perpendicular to the assumed preferred chain orientation with respect to the polarisation of the laser. Some of the spectra are highly polarised, much more than those obtained by the FT Raman measurement (Fig. 1). This is caused due to two reasons:

(1) Because of strong focusation of the laser beam in the micro-Raman confocal spectrometer, the information comes from a limited optical volume. For our objective with magnification $50\times$ it has the dimensions of a cylinder with diameter ~4 μm and height ~2 μm. As a result, the polarisation scrambling capable of decreasing undesirably the optical anisotropy is suppressed to a great extent.

(2) The micro-Raman confocal spectroscopy makes it possible to discern the more strongly oriented skins from the less oriented cores.

Table 1
Orientation of polypropylene chains in neat polymer and in PP/PE blend

		DSC	FT Raman		Micro-Raman confocal		PPA	FTIR	Correlation[c]		Chain orientation
		c^a	I_{842}/I_{809} (0°; 90°)		$R = I_{842}/I_{809}$ (0°; 90°)	$2(R^{90} - R^0)/(R^{90} + R^0)$	f^b	c^a	$R^{90} \times c_{PPAFTIR}$	$f_{MRC}{}^d$	
Neat PP	Pressed	0.46	0.76; 0.75		0.87; 0 84	−0.03	0	0.46	0.40	−0.09	None or very weak
	Injected	0.43	0.69; 0.80	Skin	0.74; 1.16	0.44	0.17	0.46	0.53	0.21	Weak
				Core	0.75; 0.98	0.26	0.17	0.48	0.47	0.07	Weak
	Drawn	0.53	0.35; 0.67	Skin	0.13; 1.82	1.73	0.88	0.47	0.86	0.97	Strong
				Core	0.23; 1.47	1.46	0.43	0.51	0.75	0.72	Medium
PP/PE blend	Pressed	0.45	0.72; 0.74		0.90; 0.90	0	0	0.45	0.41	−0.06	None or very weak
	Injected	0.42	0.64; 0.73	Skin	0.40; 1.34	1.08	0.32	0.46	0.62	0.42	Medium
				Core	0.86; 0.91	0.06	0.04	0.51	0.46	0.05	None or very weak
	Drawn	0.52	0.49; 0.65	Skin	0.11; 1.63	1.75	0.97	0.47	0.77	0.76	Strong
				Core	0.20; 1.05	1.36	0.37	0.54	0.57	0.30	Medium

[a] Crystallinity obtained from DSC or PPA FTIR [5].
[b] Orientation function obtained from PPA FTIR, see Refs. [5,10].
[c] Correlation of micro-Raman confocal orientation data with PPA FTIR.
[d] Orientation function obtained by polarised micro-Raman confocal correlated with PPA FTIR.

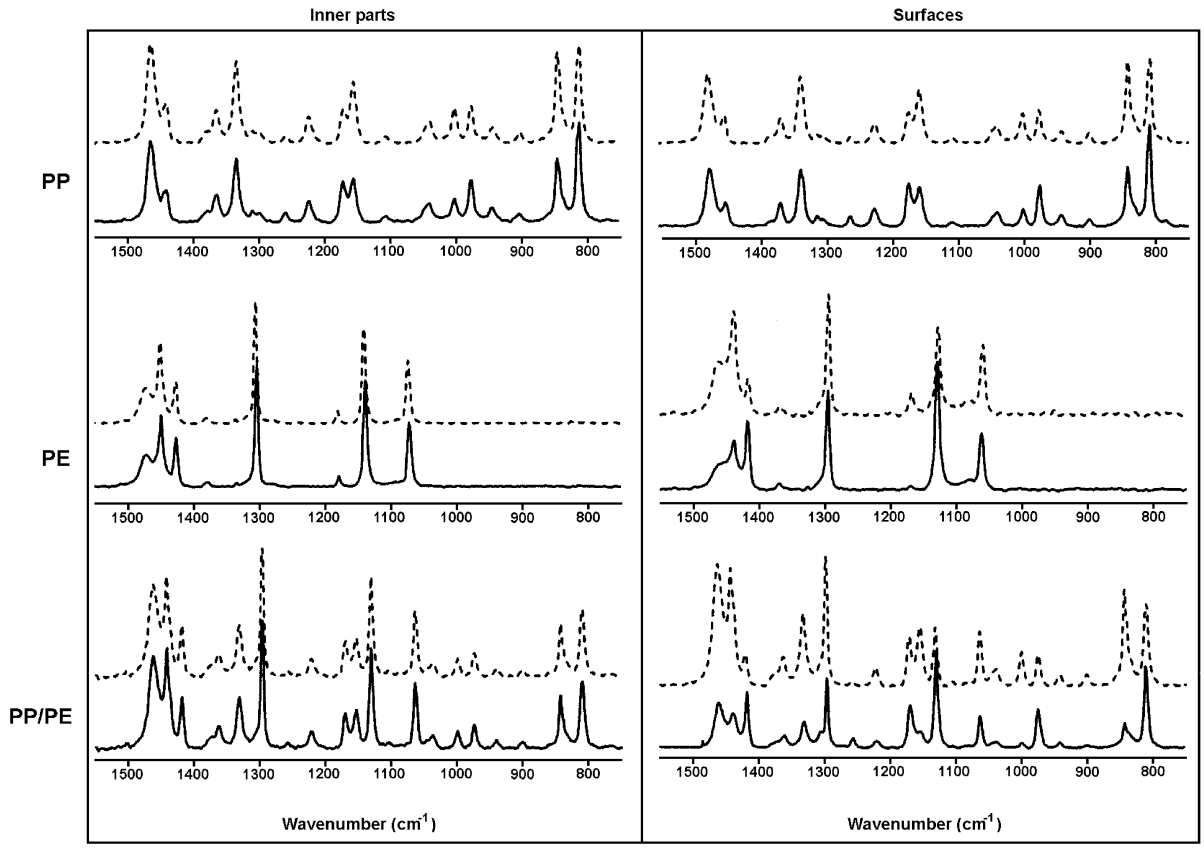

Fig. 4. Micro-Raman confocal mean spectra of injection-moulded neat PP, neat PE and PP/PE 50/50 blend measured in two opposite directions in a $100 \times 100\ \mu m^2$ square, objective magnifying $50\times$. Inner parts and surfaces. Direction of laser polarisation (—) parallel, (- - -) perpendicular to the direction of injection-moulding.

Among the 15 pairs of micro-Raman mean spectra shown in Figs. 3–5, it is possible to discern the cases with no or very weak orientation (virtually the same intensity ratio of the Raman bands measured in two opposite sample directions), the cases with weak and medium difference, and the cases with a very strong difference between the two opposite measurements.

The results of quantitative estimation are given in Table 1. It summarises the values of the DSC crystallinity and the values of the band intensity ratios I_{842}/I_{809} of the two opposite orientations as obtained from normal FT Raman spectra; then follow the band intensity ratios $R = I_{842}/I_{809}$ obtained by micro-Raman confocal measurements as 'layer' mean spectra, characterising separately the orientation in the skin and in the core.

In accordance with the facts mentioned above, polarisation scrambling influences much less the values I_{842}/I_{809} obtained by micro-Raman confocal than those obtained by normal FT Raman spectroscopy (Table 1). The value of the expression $2(R^{90} - R^0)/(R^{90} + R^0)$ (where $R = I_{842}/I_{809}$ is the ratio of the band intensity for the 0° and 90° orientation of the sample) given in the table is suitable for characterisation of the chain orientation by micro-Raman confocal. The table also shows that for the samples investigated both in the skin and in the core, the values increase roughly parallel with the values of the orientation function f obtained from polarised photoacoustic FTIR measurements (PPA FTIR) [5,10] (Table 1).

We attempted to correlate the micro-Raman confocal results with the latter orientation function more exactly. Having done this, we found that for some samples positioned at 0° between the laser polarisation and drawing, the intensity of the 842 cm^{-1} band nearly vanished (Fig. 5), which made the determination of the intensity ratios inaccurate. On the other hand, for the specimens measured at 90°, the intensities of 809 and 842 cm^{-1} bands were vanishing neither for the unoriented nor for the oriented samples, which made this position suitable for a correlation. Still, another possible obstacle had to be considered. The 809 cm^{-1} band was assigned only to the crystalline part of PP, the 842 cm^{-1} band both to the crystalline and to the amorphous part of PP [8]. As a result, the intensity ratio R depends not only on the chain orientation but, to some extent, also on the crystallinity of PP. The danger of an undesirable influence of crystallinity was considerably decreased by multiplying the values R^{90} by the crystallinity values $c_{PPAFTIR}$ obtained from PPA FTIR measurements [5] (Table 1). The resulting values $R^{90} \times c_{PPAFTIR}$ appeared to have a fairly linear correlation with the values of $f_{PPAFTIR}$

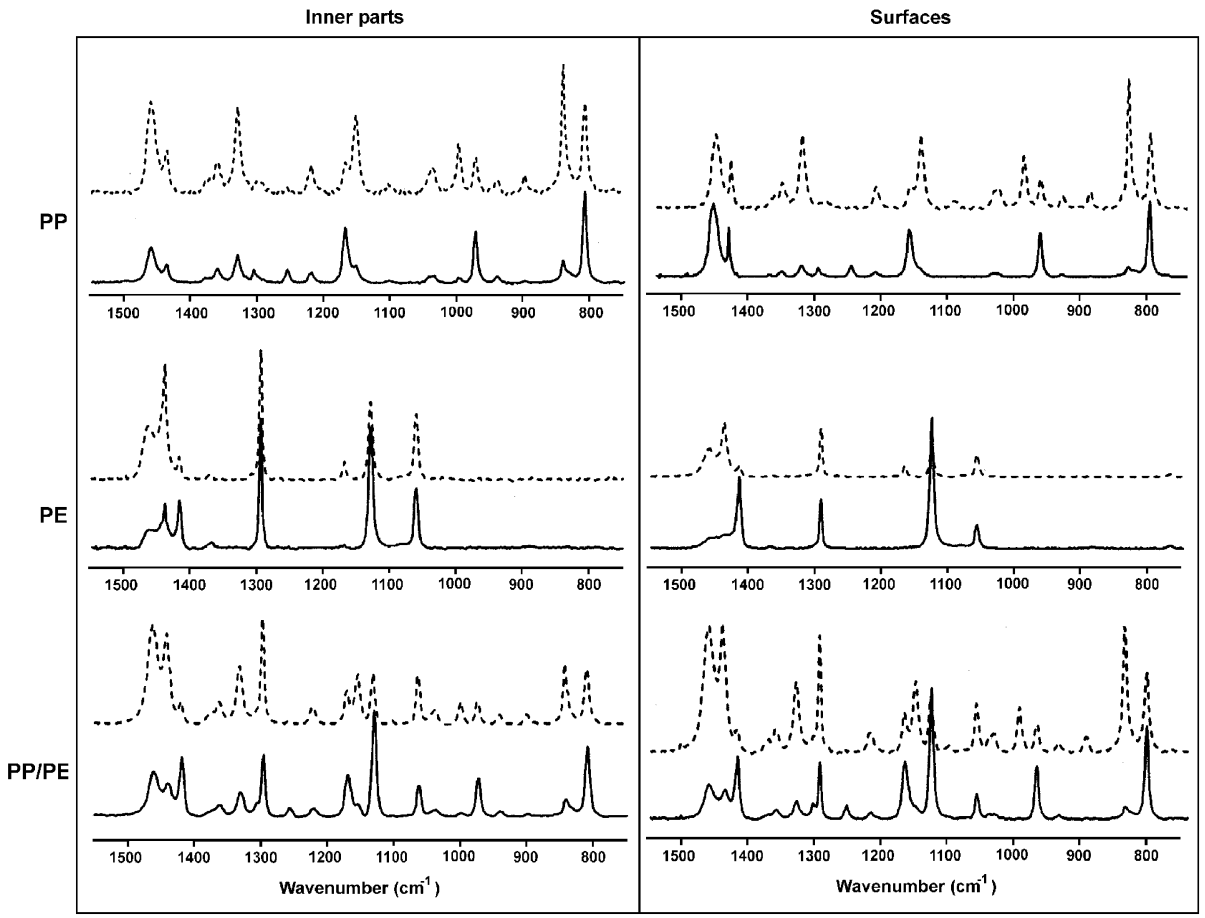

Fig. 5. Micro-Raman confocal mean spectra of injection-moulded and drawn neat PP, neat PE and PP/PE 50/50 blend measured in two opposite directions in a $100 \times 100\ \mu m^2$ square, objective magnifying $50\times$. Inner parts and surfaces. Direction of laser polarisation (—) parallel, (- - -) perpendicular to the direction of injection-moulding and drawing.

(Fig. 6). The linear relation

$$f_{MRC} = [(R^{90} \times c_{PPAFTIR}) - 0.438]/0.434 \quad (1)$$

enabled us to calculate the orientation function f_{MRC} from the micro-Raman confocal spectroscopic measurements (Table 1).

The last column of Table 1 illustrates the PP chain orientation of the investigated specimens in the neat PP and in the PP/PE blend, in accordance with the apparent view of the pairs of spectra of oppositely oriented samples in Figs. 3–5. There is no or only very weak preferred orientation both in the pressed samples and in the core of the injection-moulded PP/PE blend and only weak orientation both in the skin and in the core of neat injection-moulded PP. Medium orientation can be found in the skin of injection-moulded PP/PE blends and in the cores of drawn neat PP and drawn PP/PE blends, strong chain orientations exist in the skin of the drawn samples, both of PP and of PP/PE blend. As a result, the micro-Raman confocal spectroscopy characterised well the PP chain orientation of

Table 2
Degree of orientation of PP microdomains in PP/PE blends determined by micro-Raman confocal spectroscopy

Sample	$c_{PPAFTIR}$	Microdomain[a]	R^{90}	$R^{90} \times c_{PPAFTIR}$	f_{MRC}[b]	θ[c]
Pressed blend	0.45	Maximum	0.98	0.44	0.03	53
		Mean	0.90	0.41	−0.06	57
		Minimum	0.84	0.38	−0.13	60
Drawn blend (core)	0.54	Maximum	1.17	0.63	0.44	38
		Mean	1.05	0.57	0.30	43
		Minimum	0.91	0.49	0.12	50

[a] Microdomains are characterised by values of the ratio $R^{90} = I_{842}/I_{809}$.
[b] Orientation function obtained from micro-Raman confocal after correlation with PPA FTIR.
[c] Angle θ calculated from the orientation function f_{MRC} using Eq. (2).

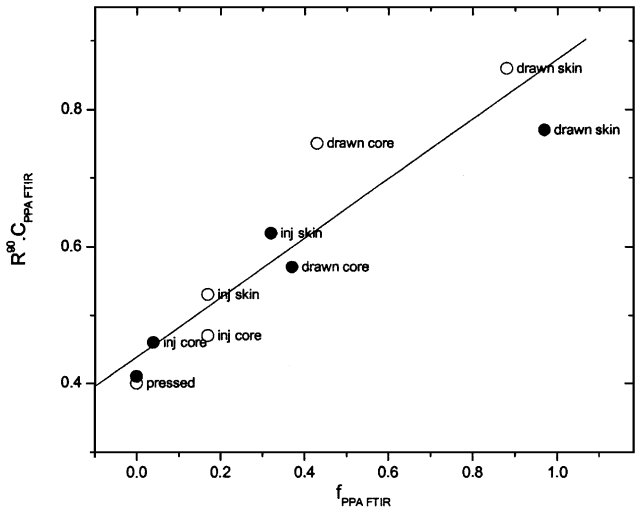

Fig. 6. Correlation of the orientation data results of micro-Raman confocal with the orientation function obtained by PPA FTIR (see the text and Table 1). ○ neat PP, λ PP in blend.

differently prepared specimens, confirming the results obtained by PPA FTIR [5].

As to the chain orientation of PE [9], it is also clearly reflected in the micro-Raman confocal spectra (Figs. 4 and 5). From the figures it follows that the orientation of PE chains is larger in the skin of injection-moulded and of drawn samples than in their cores. Nevertheless, the possible direction of PE chains of differently prepared and treated specimens both in the neat polymer [11] and in the blend [5,12] is more complex. Because of this, the PE chain orientation is not discussed in this article in more detail.

3.2.2.2. Estimation of chain orientation in different domains. As mentioned above, the orientation of polymer specimens was not homogeneous. Spectra of some of the specimens revealed a 'chain orientation microstructure'—changes in orientation at different sites of a specimen. The domains larger than 15 μm with sufficiently different orientation existed there and the micro-Raman confocal spectra enabled us to characterise them. The effect is documented in Fig. 7, showing the parts of spectra of the compression-moulded blend (Fig. 7(a)) and of the core of the drawn PP/PE blend measured at 90° (Fig. 7(b)). Each sample is characterised by the mean spectrum derived by averaging the measurements of the square 100 μm × 100 μm and by the spectra taken in the two found positions of this square where the differences in the $R = I_{842}/I_{809}$ ratios were extreme. It follows from the figures that the differences in the intensity ratios of 809 and 842 cm^{-1} bands are quite pronounced. Similarly to Table 1, Table 2 shows the values of f_{MRC} for orientation in different domains, using the relation (1). The average angles Θ of PP chain with respect to drawing axes are also calculated here using the expression derived in Ref. [13]

$$f_{MRC} = (3\cos^2\theta - 1)/2 \qquad (2)$$

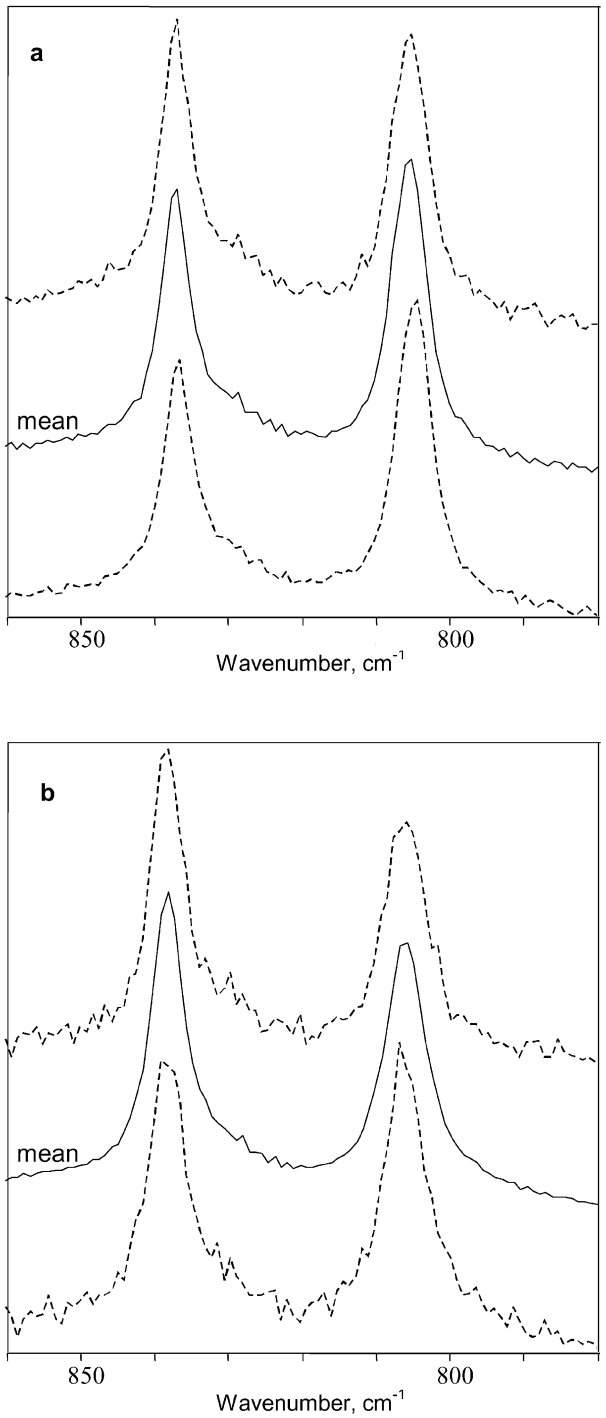

Fig. 7. Domain orientation of PP/PE blend. Spectra obtained from the 100 × 100 μm^2 square. Objective magnifying 50 ×. (a) Compression-moulded specimen, (b) core of drawn specimen, laser polarisation 90° with respect to drawing. (—) are the mean spectra, (- - -) are the selected spectra obtained in chosen positions with the largest differences of orientation.

It follows from Table 2 that in the compression-moulded sample (where no preferred orientation can be assumed) some domains exist with the chain axes differing by ~7° (compare Fig. 5(a)). For the sample partially oriented by drawing, such difference reaches ~12° (Fig. 5(b)). These results demonstrate the existence of fluctuations in polymer

chain orientation between individual domains of a given sample.

4. Conclusions

Micro-Raman confocal spectroscopy of differently prepared PP/PE blend specimens enabled us to discern the PP and PE microdomains and to differentiate between the domain structure in the skin and in the core. Such results cannot be achieved by other methods.

It was found that the surfaces (skin) of injection-moulded specimens cooled more rapidly during the injection-moulding exhibit markedly finer polymer domain structure than their inner parts (core) and the specimens prepared by compression moulding, where separate coalescence of the polymer drops could proceed.

By micro-Raman confocal spectroscopy, the chain orientation on the surface and in the inner part of the material was separately characterised. The undesirable scrambling effect often found in normal macro-Raman measurements is almost eliminated here. The results obtained by averaging the micro-Raman confocal spectra agree well with the results of polarised photoacoustic spectroscopy, namely with the fact that the chain orientation is much higher on the surface than in the inner part of both the injection-moulded and of the drawn blend specimens.

The measurements made at different sites of a specimen showed the existence of microregions of size ca. 10–50 μm differing in chain orientation.

All these findings are important for structure characterisation of polymer blends and for its correlation with their mechanical behaviour.

Acknowledgments

The authors are greatly indebted to the Grant Agency of the Czech Republic (grant nos. 106/97/1071, 106/02/1249) and to CICYT (MAT1999-1029) for financial support. Thanks are also due to Dr M. Raab of the Institute for helpful discussions.

References

[1] Markwort L, Kip B. J Appl Polym Sci 1996;61:231.
[2] Schmidt P, Fernandez MR, Pastor JM, Roda J. Polymer 1997;38:2067.
[3] Fernandez MR, Merino JC, Gobernado-Mitre MI, Pastor JM. Appl Spectrosc 2000;54:1105.
[4] Schmidt P, Kolařík J, Lednický F, Dybal J, Lagarón JM, Pastor JM. Polymer 2000;41:4267.
[5] Schmidt P, Dybal J, Ščudla J, Kratochvíl J, Eichhorn KJ, Quintana SL, Pastor JM. Macromol Symp, ESOPS XIV Dresden 2002; in press.
[6] Raab M, Kotek J, Baldrian J, Grellmann W. J Appl Polym Sci 1998;69:2255.
[7] Van Krevelen DW. Properties of polymers. Amsterdam: Elsevier; 1990.
[8] Arrubarrena de Baez M, Hendra PJ, Judkins M. Spectrochim Acta A 1995;51:2117.
[9] Bentley PA, Hendra PJ. Spectrochim Acta A 1995;51:2125.
[10] Schmidt P, Raab M, Kolařík J, Eichhorn KJ. Polym Test 2000;19:205.
[11] Aggarwal SL, Tilley GP, Sweeting OJ. J Appl Polym Sci 1959;1:91.
[12] Schmidt P, Baldrian J, Ščudla J, Dybal J, Raab M, Eichhorn KJ. Polymer 2001;42:5321.
[13] Hermans PH. Contributions to the physics of cellulosic fibres. Amsterdam: Elsevier; 1946. p. 138.